

\mathcal{L}_1 Adaptive Resonance Ratio Control for Series Elastic Actuator with Guaranteed Transient Performance^{*,**}

Feiyan Min^{a,*}, Gao Wang^a and Xueqin Chen^{b,**}

^aElectronic engineering department, Jinan University, 510632, Guangzhou, China

^bSchool of Astronautics, Harbin Institute of Technology, 150001, Harbin, China

ARTICLE INFO

Keywords:

Series elastic actuator
 \mathcal{L}_1 adaptive control
Resonance ratio control
Transient performance

ABSTRACT

To eliminate the static error, overshoot, and vibration of the series elastic actuator (SEA) position control, the resonance ratio control (RRC) algorithm is improved based on \mathcal{L}_1 adaptive control(LIAC)method. Based on the analysis of the factors affecting the control performance of SEA, the algorithm schema is proposed, the stability is proved, and the main control parameters are analyzed. The algorithm schema is further improved with gravity compensation, and the predicted error and reference error is reduced to guarantee transient performance. Finally, the effectiveness of the algorithm is validated by simulation and platform experiments. The simulation and experiment results show that the algorithm has good adaptability, can improve transient control performance, and can handle effectively the static error, overshoot, and vibration. In addition, when a link-side collision occurs, the algorithm automatically reduces the link speed and limits the motor current, thus protecting the humans and SEA itself, due to the low pass filter characterization of LIAC to disturbance.

1. Introduction

The series elastic actuator (SEA) was first proposed by Parrt in 1995 [1], which can reduce the contact stiffness between the manipulator and the environment or human, to ensure the safety and adaptability of interactive operation for manipulators. However, the introduction of series elastic actuators may increase the complexity of the robot dynamics model, deteriorate the transient performance, and lead to mechanical resonance, overshoot, and static error on the link side.

Series elastic actuators provide valuable properties compared to rigid joints [2]. First, the mechanical output impedance of the flexible joint is reduced, helping to establish a stable contact between the load and the motor output shaft. Second, the elastic element can absorb the energy impact generated by the accidental collision, reducing the peak moment of the collision and thus the impact on the mechanical structure. Third, elastic components can store mechanical kinetic energy, allowing higher peak power output. Fourthly, the elastic components can be used as a torque sensor due to the better linearity between the torsion angle and the output torque.

However, the position and force control of SEA is more complicated [3]. First of all, compared with the rigid structure, the dynamic model of SEA is more complex; the order of the model increases from 2 to 4, and the difficulty of stability and accuracy increase significantly. Furthermore, the elastic components are easy to cause vibration, which makes the link side still have residual jitter when it reaches the target

position. Third, passive flexibility dramatically reduces the system's control bandwidth and limits the tracking ability.

Motion control of SEA is regarded as an essential issue in the next generation of industrial robots. Consequently, since the 1990s, the research of its control problem has become the focus of attention, and various control methods have been proposed.

Spong[4][5] et al. proposed a simplified linear model of a flexible joint robot, and various control methods based on this model were researched. Tomei[6] successively proposed the PD control method and gravity compensation control strategy and proved the closed-loop stability condition. Although the PD control algorithm can guarantee convergence, there is no better demonstration of steady-state error and vibration.

Kouhei Ohnishi [7] [8] et al. proposed the Disturbance Observer (DOb) and Resonance Ratio Control (RRC) algorithm, which had a great attention. Among them, the disturbance observer is very effective in compensating for the friction of the motor side and has become a common algorithm for servo motors and industrial robot. The Resonance Ratio Control includes position control mode and force control mode [9][10][11]. The idea is that through the state feedback of the motor side and the link side, the closed-loop poles are configured so that there are no conjugate poles, and the system response is non-oscillating. However, the algorithm assumes that the model and the external interference is precisely known, of which the latter is often difficult to satisfy.

In addition, a variety of control algorithms are proposed. The most common is the so-called linear model based control methods, including the Extended state observer (ESO) [12] and feedback linearization [13], etc. Sun Lei [14][15] et al. proposed a controller with a non-linear structure to achieve effective suppression of overshooting and vibration, which was verified on a multi-link manipulator. And Daniel et al. propose the fractional-order control method for flexible joint robot[16].

* This work was supported in part by the National Natural Science Foundation of China under Grant 62172188

*Corresponding author: Feiyan Min. E-mail address: feiyan.min@jnu.edu.cn

**Co-corresponding author: Xueqin Chen. E-mail address: cxqh163@163.com

ORCID(s):

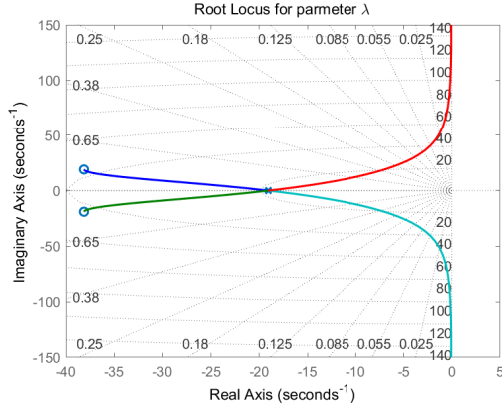


Figure 2: Parametric root locus for different contact stiffness

where $\Delta = -(s^2 + 4\omega s + 5\omega^2)\Delta G/J_a$, $\rho_0 = -(s^2 + 4\omega s + 5\omega^2)K_e q_0/J_a$, and close loop characteristic equation $Q(s) = s^4 + 4\omega s^3 + (6\omega^2 + \lambda)s^2 + (4\omega^3 + 4\omega\lambda)s + (\omega^4 + 5\lambda\omega^2)$, $\lambda = K_e/J_a$.

The parameter root locus with respect to λ is shown in the figure 2. Conjugate poles appear when $\lambda > 0$, so the overshoot and vibration increases with the increase of K_e . Meanwhile, the mass uncertainty ΔG will introduce the steady-state error of the closed-loop response.

3. \mathcal{L}_1 Adaptive motion control

As discussed above, the main interference is located in the link side, while the drive is the motor side, this is an unmatched system. For this structure, we adopt the piecewise discrete adaptive law in \mathcal{L}_1 controller design, which is based on linear state space model.

However, the nonlinear term gravity cannot be involved in the linear model, and is ignored as disturbance in the initial design. And then we improve the structure of controller with an online nonlinear gravity compensation algorithm, and the stability and tracking performance of the control algorithm are analyzed.

3.1. \mathcal{L}_1 Adaptive resonance ratio control law

The starting \mathcal{L}_1 adaptive motion control system is given by the following equation:

$$\begin{cases} \dot{x}(t) &= Ax(t) + B_m(u(t) + \sigma_1(t)) + B_{um}\sigma_2(t) \\ x(0) &= x_0 \\ y(t) &= cx(t) \end{cases} \quad (7)$$

where $x(t) \in R^n$ is the state vector of the system. A is constant system matrix, $B_m \in R^{n \times m}$ is the control channel matrix, $u(t)$ is the control signal, σ_1 is the disturbance matched with B_m . σ_2 is the unmatched disturbance with channel matrix $B_{um} \in R^{n \times (n-m)}$, and $\text{rank}([B_m, B_{um}]) = n$.

The control structure is given as follows:

$$u(t) = u_1(t) + u_2(t) \quad (8)$$

where $u_1(t) = -Kx(t)$ is the state feedback control law designed for the nominal system to realize poles assignment, and the value of K is required to make $A_m = A - B_m K$ Hurwitz.

Obviously, the RRC mentioned above is transformed into the state feedback control law $u_1(t)$. The state variable is chosen as $x = [q, \dot{q}, \theta, \dot{\theta}]'$, and the control law in (2) is transformed as

$$K = [-K_r K_f, 0, K_p + K_r K_f, K_v] \quad (9)$$

where the nonlinear term G is ignored in linear state feedback controller design. That means the gravity is considered as unknown disturbance in total and will be compensated in the adaptive control law $u_2(t)$. And the state equation is

$$\begin{cases} \dot{x} = A_m x + B_m(u_2 + \sigma_1) + B_{um}\sigma_2 \\ A_m = \begin{bmatrix} 0 & 1 & 0 & 0 \\ -\frac{K_f}{J_a} & 0 & \frac{K_f}{J_a} & 0 \\ 0 & 0 & 0 & 1 \\ K_r K_f & 0 & -K_r K_f - K_p & -K_v \end{bmatrix} \\ B_m = \begin{bmatrix} 0 \\ 0 \\ 0 \\ 1 \end{bmatrix} & B_{um} = \begin{bmatrix} 1 & 0 & 0 \\ 0 & 1 & 0 \\ 0 & 0 & 1 \\ 0 & 0 & 0 \end{bmatrix} \end{cases} \quad (10)$$

The adaptive control law $u_2(t)$ compensates the disturbance of σ_1, σ_2 and tracks the target link side position q_d .

The disturbance above is assumed to be bounded and verifies following condition:

Assumption 1: σ_1 a scalar, there exist L_1, B_1 such that

$$\|\sigma_1\|_\infty \leq L_1 \|x\|_\infty + B_1 \quad (11)$$

Assumption 2: $\sigma_2 = [\sigma_{21}, \sigma_{22}, \sigma_{23}]'$ is a three dimension column vector, and there exist L_2, B_2 such that

$$\|\sigma_2\|_\infty \leq L_2 \|x\|_\infty + B_2 \quad (12)$$

Remark 1. Among the four disturbances $\sigma_1, \sigma_{21}, \sigma_{22}, \sigma_{23}$, the motor side disturbance σ_1 is mainly the mechanical friction τ_{fm} , and is compensated by the DOB. In contrast, the external force on the link side $\sigma_{22} = \tau_{dis}$ is the dominant disturbance for the SEA control.

To synthesize the adaptive law, it is necessary to predict the state and estimate the value of disturbance. The state predictor equation is:

$$\dot{\hat{x}} = A_m \hat{x} + B_m(u_2(t) + \hat{\sigma}_1) + B_{um}\hat{\sigma}_2 \quad (13)$$

where $\hat{x}, \hat{\sigma}_1, \hat{\sigma}_2$ is the predicting value of x, σ_1, σ_2 , respectively.

The adaption law estimates the matched disturbance σ_1 and unmatched disturbance σ_2 , and the computational equa-

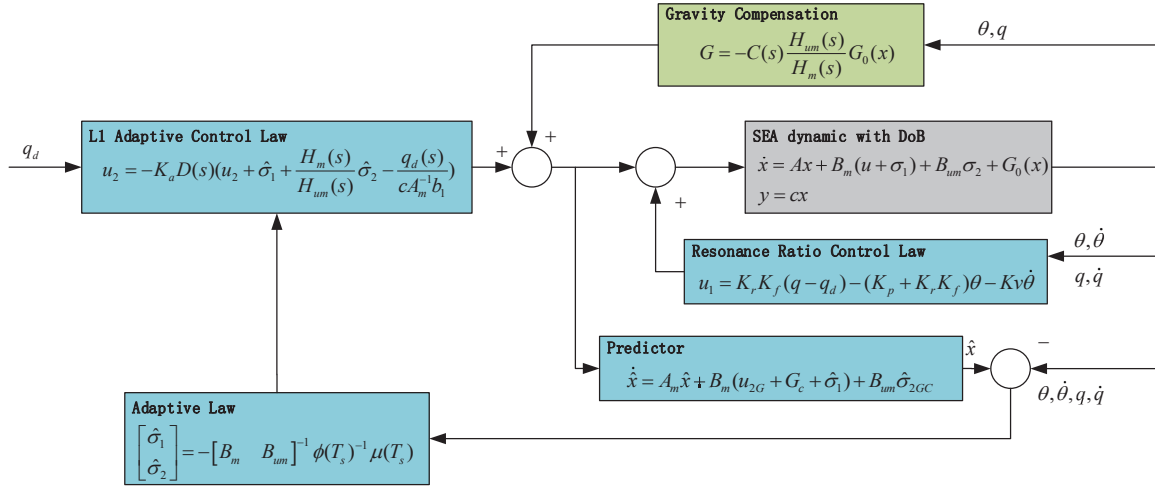


Figure 3: \mathcal{L}_1 Adaptive Resonance Ratio Control for SEA

tion is as:

$$\begin{cases} \tilde{x}(iT_s) = \hat{x}(iT_s) - x(iT_s) \\ \mu(T_s) = e^{A_m T_s} \tilde{x}(iT_s) \\ \phi(T_s) = A_m^{-1} (e^{A_m T_s} - I_n) \\ \begin{bmatrix} \hat{\sigma}_1((i+1)T_s) \\ \hat{\sigma}_2((i+1)T_s) \end{bmatrix} = -[B_m B_{um}]^{-1} \phi(T_s)^{-1} \mu(T_s) \end{cases} \quad (14)$$

where \tilde{x} is the predict error, and T_s is adaption rate.

The adaptive control law $u_2(t)$ is updated with follow algorithm:

$$u_2 = -\frac{K_a D(s)}{(I_m + K_a D(s))} (\hat{\sigma}_1 + H_m^{-1}(s) H_{um}(s) \hat{\sigma}_2 - K_g q_d(s)) \quad (15)$$

where the matrices $H_m(s)$, $H_{um}(s)$ and K_g are defined as

$$\begin{aligned} H_m(s) &= c(sI_n - A_m)^{-1} B_m \\ H_{um}(s) &= c(sI_n - A_m)^{-1} B_{um} \\ K_g &= -(cA_m^{-1} B_m)^{-1} \end{aligned} \quad (16)$$

The tuning parameters include the low-pass filter $D(s)$ control gain K_a , they have to be chosen such that:

$$C(s) = K_a D(s) (I_m + K_a D(s))^{-1} \quad (17)$$

is stable and has DC gain $C(0) = I_m$; furthermore $C(s)H_m^{-1}$ has to be a strictly proper transfer function.

3.2. Stability and Transient Performance

Reference system is constructed for the proof of stability and transient performance of \mathcal{L}_1 adaptive control system. The reference system assumes perfect identification of all uncertainties, and cancel them within the bandwidth of the low pass filter $C(s)$. It should be noted that this auxiliary

reference system is not implementable, and not involved in the implementation of the \mathcal{L}_1 adaptive control system.

$$\begin{cases} \dot{x}_r = A_m x_r + B_m(u_{2r} + \sigma_{1r}) + B_{um}\sigma_{2r} \\ u_{2r}(s) = -C(s)(\sigma_{1r} + H_{mum}(s)\sigma_{2r} - K_g q_{dr}) \end{cases} \quad (18)$$

where $u_{2r}(s)$ is the Laplace transform of the adaptive control law u_2 , $H_{mum}(s) = H_m^{-1}(s)H_{um}(s)$, $x_r = [q_r, \dot{q}_r, \theta_r, \dot{\theta}_r]$ is the state variable of reference system. σ_{1r} and $\sigma_{2r} = [\sigma_{21r}, \sigma_{22r}, \sigma_{23r}]'$ is the identified disturbance in the reference system.

The close loop transfer function of reference system is

$$x_r(s) = G_1(s)\sigma_{1r} + G_2(s)\sigma_{2r} - G_d(s)K_g q_{rd} \quad (19)$$

where $G_1(s) = (sI_n - A_m)^{-1} B_m(1 - C(s))$, $G_2(s) = (sI_n - A_m)^{-1} B_{um}(1 - C(s))$, $G_d = (sI_n - A_m)^{-1} B_m C(s)$

For the proof of stability and transient performance bound of reference system, the choice of K_a and $D(s)$ also needs to ensure that, there exists bounded positive ρ_r such that the following condition holds:

$$\|G_1\|_{L_1} l_0 + \|G_2\|_{L_1} < \frac{\rho_r + \|G_d\|_{L_1} \|q_{dr}\|_{\infty}}{L_2 \rho_r + B_0} \quad (20)$$

where $l_0 = L_1/L_2$, $B_0 = \max(B_1/l_0, B_2)$

Lemma 1. For the close loop reference system (18), subject to the condition(20), then

$$\|x_r\|_{\infty} \leq \rho_r \quad (21)$$

Lemma 2. For the prediction equation (13), (14), if there exists a time τ such that truncation function $\|\tilde{x}_{\tau}\|_{\infty}$ is bounded. then

$$\|\tilde{x}_{\tau}(t)\|_{\infty} \leq \Gamma \quad (22)$$

where $\Gamma = (\alpha_1(T_s) + \alpha_2(T_s))\gamma_0 + \alpha_3(T_s)\gamma_1 + \alpha_4(T_s)\gamma_2$

Theorem 1. Given the close loop system via (7)~(10), and the reference system in (18), if the condition is (20) holds, then

$$\|x_r - x\|_{\infty} < \Gamma_r \quad (23)$$

Table 1
SEA system parameters.

System parameters	Actual value	Unit
Motor side inertia	$J_m = 0.294$	kgm^2
Link side inertia (With nominal load)	$J_a = 0.345$	kgm^2
Spring stiffness	$K_f = 125.478$	Nm/rad
Load torque($q = 90^\circ$) (With nominal load)	$G_0 = 8.856$	Nm
Nominal load	$m_0 = 1.5$	kg
Test load	$m = 0.5, 1.5, 2.0$	kg
Motor torque coefficient	$K_t = 0.094$	$Nm/\%o$
Viscous coefficient	$f_m = 4.082$	$Nm/(rad/s)$
Natural frequency	$\omega = 19.068$	rad/s
Parameter of DoB	$g_{ob} = 500$	rad/s

where $\Gamma_r = \frac{\|G_d(s)H_m^{-1}(s)\|_{L1}}{1 - \|G_1(s)\|_{L1}L_1 - \|G_2(s)\|_{L1}L_2} \Gamma + \epsilon$, and ϵ is an arbitrarily small positive constant.

Remark 3. The bound of reference error Γ_r is also affected by the uncertainties and external disturbances σ_1 and σ_2 , and can be reduced with small enough sampling time T_s .

4. Controller Design

This section designs a SEA controller based on the L1 adaptive control algorithm proposed above and compares it with the standard RRC control algorithm by simulation. Figure 4 shows the SEA test platform, and table 1 shows the relevant parameters. In order to test the adaptability of the algorithm to load changes, we add variable load to nominal link inertia. On the other hand, a collision test platform with variable stiffness is built to test the response characteristics of the position control algorithm under environmental collision.

The controller (8) includes state feedback control law u_1 and adaptive control law u_2 . The u_1 adopts the control parameter of the standard RRC, as shown in (2) and (9). The u_2 form is as in (15), and the designed parameters include the adaptive gain K_a and the low-pass filter $D(s)$, which ensure that (17) is stable and $C(s)H_m^{-1}(s)$ is strictly proper. Since the SEA system is a fourth-order system, the candidate $D(s)$ are as follows

$$D(s) = \frac{1}{s(Ts + 1)^3} \quad (24)$$

where T is the time constant of the filter. Since the sampling rate of the control system is $T_s = 0.001s$, T should be greater than this value. Therefore, $T = 0.005, 0.01, \text{ and } 0.02s$ is selected for the test.

5. Conclusion

This paper proposes a SEA control algorithm based on L1AC with a gravity compensation algorithm to improve the transient control performance. The main disturbance is located in the link side, while the drive is the motor side, this is

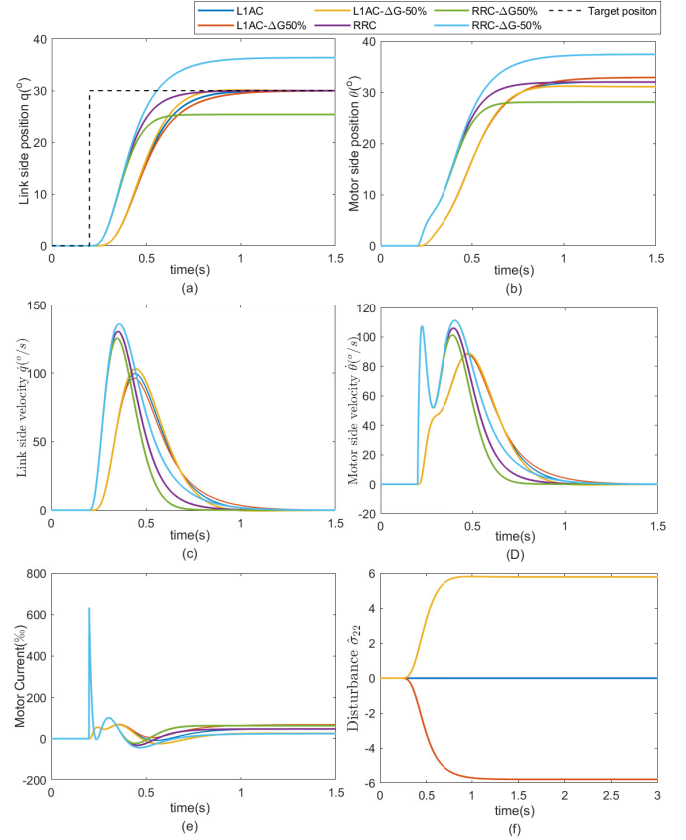


Figure 4: Simulation results under load variation. The nominal mass is 1.5kg, and simulation experiments with loads of 0.75kg, 1.5kg, and 2.25kg are carried out using L1AC and RRC algorithms, respectively. The L1AC algorithm has no static error, but RRC has a sizeable static error. The response speed of L1AC is slow by 0.1s due to the influence of LPF $C(s)$, but there is no spike current in this algorithm, as in (e). $\hat{\sigma}_{22}$ in (f) is the estimate of the disturbance torque on the link side, which, multiplied by related coefficients, is the actual estimate of the external disturbance. (The unit of motor current is one thousandth of the nominal current)

an unmatch system, and the piecewise discrete adaptive law is used, which is based on linear state space model. So the nonlinear term gravity is ignored as disturbance in the initial design. And then we improve the structure of controller with an online nonlinear gravity compensation algorithm, and the stability and tracking performance of the control algorithm are analyzed.

CRediT authorship contribution statement

Feiyan Min: Conceptualization of this study, Methodology, Software, Writing. **Gao Wang:** Experiment. **Xueqin Chen:** Data curation, Supervision.

References

- [1] G. A. Pratt and M. M. Williamson. "series elastic actuators," in proceedings 1995 ieee/rsj international conference on intelligent robots

- and systems. *Human Robot Interaction and Cooperative Robots (Pittsburgh, PA: IEEE)*, page 525827, 1995.
- [2] N. Paine, S. Oh, and L. Sentis. Design and control considerations for high-performance series elastic actuators. *IEEE-ASME TRANSACTIONS ON MECHATRONICS*, 19:1080–1091, 2014.
 - [3] A. Calanca, R. Muradore, and P. Fiorini. A review of algorithms for compliant control of stiff and fixed-compliance robots. *IEEE-ASME TRANSACTIONS ON MECHATRONICS*, 21:613–624, 2016.
 - [4] M. W. Spong. Modeling and control of elastic joint robots. *Journal of Dynamic Systems, Measurement, and Control*, 1987.
 - [5] M. W. Spong. Control of flexible-joint robots: A survey. *Control Systems Laboratory, University of Illinois at Urbana-Champaign*, 1990.
 - [6] P. Tomei. Adaptive pd controller for robot manipulators. *IEEE Transactions on Robotics and Automation*, 7:565–570, 1991.
 - [7] K. Yuki, T. Murakami, and K. Ohnishi. Vibration control of 2 mass resonant system by resonance ratio control. *Conference of the IEEE Industrial Electronics Society IEEE Xplore*, 1993.
 - [8] E. Sariyildiz and K. Ohnishi. An adaptive reaction force observer design. *IEEE/ASME Transactions on Mechatronics*, 2014.
 - [9] Thao, Tran Phuong, K. Ohnishi, and Y. Yokokura. Fine sensorless force control realization based on dither periodic component elimination kalman filter and wide band disturbance observer. *IEEE Transactions on Industrial Electronics*, pages 1–1, 2018.
 - [10] C. Mitsantisuk, K. Ohnishi, and S. Katsura. design for sensorless force control of flexible robot by using resonance reaction control based coefficient diagram method. *ATKAFF*, pages 62–73, 2013.
 - [11] E. Sariyildiz. Acceleration measurement enhances the bandwidth of disturbance observer in motion control systems. 2021.
 - [12] S. E. Talole and S. B. Phadke. Extended state observer based control of flexible joint system. *IEEE International Symposium on Industrial Electronics*, 2008.
 - [13] A. D. Luca and P. Lucibello. A general algorithm for dynamic feedback linearization of robots with elastic joints. *Robotics and Automation*, 1998.
 - [14] Li P, Sun L, Zhao W, and et al. Position control of flexible joint robots with pd controller based on disturbance observer. 2019.
 - [15] L Sun, W Yin, and JT Liu. Position control for flexible joint robot based on online gravity compensation with vibration suppression. *IEEE TRANSACTIONS ON INDUSTRIAL ELECTRONICS*, 65:4840–4848, 2018.
 - [16] Daniel Feliu-Talegon, Vicente Feliu-Batlle, I. Tejado, Blas M. Vinaigre, and S. Hassan HosseinNia. Stable force control and contact transition of a single link flexible robot using a fractional-order controller. *ISA Transactions*, 89:139–157, 2019.
 - [17] Mohammad Javad Fotuhi and Zafer Bingul. Fuzzy torque trajectory control of a rotary series elastic actuator with nonlinear friction compensation. *ISA Transactions*, 115:206–217, 2021.
 - [18] Cao C and Hovakimyan N. L1 adaptive output feedback controller for non strictly positive real multi-input multi-output systems in the presence of unknown nonlinearities. 2009.
 - [19] E. Xargay, N. Hovakimyan, and C. Cao. L1 adaptive controller for multi-input multi-output systems in the presence of nonlinear unmatched uncertainties. *Proceedings of the 2010 American Control Conference*, pages 874–879, 2010.
 - [20] H Lee, V Cichella, and N Hovakimyan. L1 adaptive output feedback control for underactuated mimo systems. *IFAC-Papers Online*, 2017.
 - [21] CY Cao and N Hovakimyan. Stability margins of l-1 adaptive control architecture. *IEEE TRANSACTIONS ON AUTOMATIC CONTROL*, 55:480–487, 2010.
 - [22] Bing, Sun, Man, and et al. A cascaded adaptive uuv tracking control design with ocean current.
 - [23] RS Zhu, GF Yin, and ZL Guo. Temperature control of cryogenic wind tunnel with a modified l-1 adaptive output feedback control. *MEASUREMENT AND CONTROL*, 51:498–513, 2018.
 - [24] Qinmin Yang, Xuguo Jiao, Qingshun Luo, Qi Chen, and Youxian Sun. L1 adaptive pitch angle controller of wind energy conversion systems. *ISA Transactions*, 103:28–36, 2020.
 - [25] Zongyu Zuo, Xiao Li, and Zhiguang Shi. L1 adaptive control of un-
- certain gear transmission servo systems with deadzone nonlinearity. *ISA Transactions*, 58:67–75, 2015.